Finite-size effects in the phonon density of states of nanostructured germanium: A comparative study of nanoparticles, nanocrystals, nanoglasses, and bulk phases

D. Şopu,* J. Kotakoski,† and K. Albe

Institut für Materialwissenschaft, Technische Universität Darmstadt, Petersenstrasse 32, D-64287 Darmstadt, Germany

(Received 23 February 2011; revised manuscript received 22 April 2011; published 22 June 2011)

Finite-size effects in the phonon density of states (PDOS) of nanostructured materials (nanoparticles, nanocrystals, embedded nanoparticles, and nanoglasses) are systematically studied by means of molecular dynamics simulations, where germanium was used as representative reference material. By comparing with the PDOS of single crystalline and amorphous structures, the physical origins of additional or vanishing vibrational modes or frequency shifts were identified. Our findings are discussed in terms of phonon confinement effects, structural disorder, and surface stresses and provide a general view on the interplay of nanostructural features and lattice vibrations.

DOI: 10.1103/PhysRevB.83.245416 PACS number(s): 63.22.−m, 68.03.Cd, 63.70.+h, 83.10.Rs

I. INTRODUCTION

Phonons generally affect the thermal, optical, mechanical, and electrical properties of materials. While the phonon density of states (PDOS) is primarily a function of the local atomic structure, it is also sensitive to atomic-level stresses and the microstructure. If the characteristic length scales get down to the nanometer regime, deviations of the PDOS from the corresponding bulk structure have been observed, both in experiment and theory.[1–6] The microscopic origins of the observed size effects are, however, very often not clear.

Size effects due to the variation of the surface to volume ratio are expected to scale with $D^{-\alpha}$ ($\alpha \approx 1$),[7] where D describes the intrinsic structural length, like grain or particle diameter. Phonon confinement due to finite particle size[8] or quantum phenomena originating from the discreteness of electron states and band-gap variation with nanostructure size,[9] both scale with D^{-2}. The presence of grain boundaries (GBs)[1,4,10,11] or surfaces[7] leads to a locally lower atomic density and higher structural disorder in comparison to the bulk material resulting in additional vibrational modes at low and high frequencies.[5] Confinement effects affect the optical modes at the Brillouin zone center ($q = 0$), since more phonons with $q \neq 0$ (away from Brillouin zone center) contribute to the PDOS and lead to a redshift in Raman spectra.[2,8,12] This has been reported for different nano-scale materials like nanocrystals,[2,12,13] nanoparticles embedded in glass,[3,14] or other nanostructures.[15] The redshift observed in Raman spectra, however, has also been explained by tensile surfaces stresses,[16] while the blueshift has been attributed to compressive surface stresses (or pressure).[17] This interpretation was supported by atomistic simulations[7] that revealed the influence of surface stresses on the PDOS, resulting in a shift of the entire PDOS toward higher frequencies for the case of metals.

In view of the partially controversial interpretation of the PDOS of nanostructured materials, a detailed study revealing the role of the various size effects appears to be a worthwhile task. In this study, we calculate the PDOS separately for nanoparticles, nanocrystals, nanoparticles embedded in a glass, and a nanoglass, which is a class of material that is synthesized by consolidating glassy nanoparticles.[18] We determine how the vibrational modes are affected by changes in the nanostructure as compared to crystalline and amorphous bulk materials. Moreover, we show how the PDOS changes with nanoparticle size through surface stress and confinement effects. Germanium is chosen as a prototype of a covalently bonded material with crystalline and amorphous modifications. After a short description of the computational methods, we start with the case of a free crystalline nanoparticle. Then a particle embedded in a glass structure is studied, before we investigate a nanocrystalline microstructure. Finally, we discuss the case of a glass with microstructure, a so-called nanoglass, where internal planar defects are present.

II. METHODS AND COMPUTATIONAL DETAILS

Classical molecular dynamics (MD) simulations were carried using the MD code PARCAS.[19] Tersoff's interatomic potential for germanium was used in this study to represent the interactions between the atoms.[20] For comparison, some of the results were repeated using the Stillinger-Weber potential.[21]

The phonon densities of states (PDOS) were computed from the Fourier transform of the velocity autocorrelation function (VAC):[22]

$$g(\omega) = \int dt\, e^{i\omega t} \frac{\langle \vec{v}(t) \cdot \vec{v}(0) \rangle}{\langle \vec{v}(0)^2 \rangle}, \tag{1}$$

where $\vec{v}(0)$ is the average velocity vector of a particle at initial time, $\vec{v}(t)$ is the average velocity at time t, and ω is the frequency. In order to exclude the contribution of atomic rearrangements or diffusional jumps to the VAC, the system was equilibrated in an isobaric-isothermal ensemble. In consequence, all PDOS approach zero at $\omega = 0$. We calculated the average of Eq. (1) over all particles and for ten different independent cases. All PDOS calculations were performed at 50 K and for times long enough to obtain a good frequency resolution.

Using this technique, we first calculated the PDOS of Ge in a single-crystalline diamond structure (see Fig. 1, right). In order to understand the features of the PDOS, we also calculated the phonon dispersion for the diamond structure (Fig. 1, left) using the frozen phonon method.[23] Four crystalline peaks are identified in the PDOS, namely the transverse acoustic (TA), longitudinal acoustic (LA), longitudinal optical (LO),

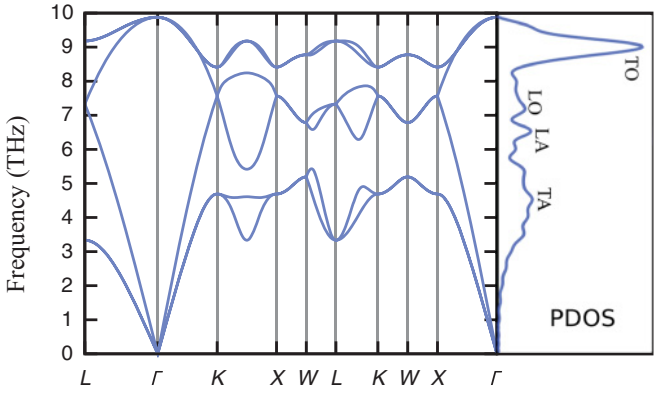

FIG. 1. (Color online) Calculated phonon dispersion for diamond Ge crystal and its calculated density of states (in arbitrary units).

and transverse optical (TO) modes, in the order of ascending energy (see Fig. 1, right).

The calculated phonon dispersion and PDOS for the Ge crystal is in fair agreement with experimental and theoretical data.[24,25] However, Tersoff-type potentials tend to overestimate the frequencies of the transverse acoustic (TA) modes at the zone boundary and also the optical modes, since this model is too stiff for angular distortions.[26] Despite this fact, the Tersoff potential is suitable for studying finite-size effects in the PDOS of nanostructured Ge on a qualitative level, since it is known to reproduce the structural properties of crystalline, liquid, and amorphous states of germanium.[27]

The PDOS can be used for determining thermodynamic properties of a material. For instance, the specific heat at constant volume C_v can be directly calculated within the harmonic approximation as

$$C_v(T) = 3k_B \int_0^{\omega_{\max}} \left(\frac{\hbar\omega}{k_B T}\right)^2 \frac{e^{\frac{\hbar\omega}{k_B T}}}{\left(e^{\frac{\hbar\omega}{k_B T}} - 1\right)^2} g(\omega) d\omega, \quad (2)$$

where $g(\omega)$ is the PDOS [see Eq. (1)], $\hbar$ the Planck's constant divided by 2π, and k_B the Boltzmann's constant.

III. RESULTS AND DISCUSSIONS

A. Free nanoparticles

In the first set of calculations, free nonsupported particles were studied, which for simplicity were created as spherical cuts of the bulk phase and relaxed at 50 K before the PDOS was analyzed. The result is shown in Fig. 2(a), where the PDOS of the single crystal is compared with the PDOS of nanoparticles with diamaters of 3.9 and 7.5 nm. Essentially, two major features can be observed, namely the broadening of the acoustical branch and a redshift of the entire distribution, which gets more pronounced as the particle size decreases. The enhancement of the acoustical modes at lower frequency can be directly attributed to the presence of weakly bonded surface atoms, characterized by a lower coordination.

By removing all atoms with a diamond-like configuration from the PDOS calculation through a common neighbor analysis,[28] it becomes obvious that additional acoustic modes are due to surface atoms [see Fig. 2(b)] only, while the presence

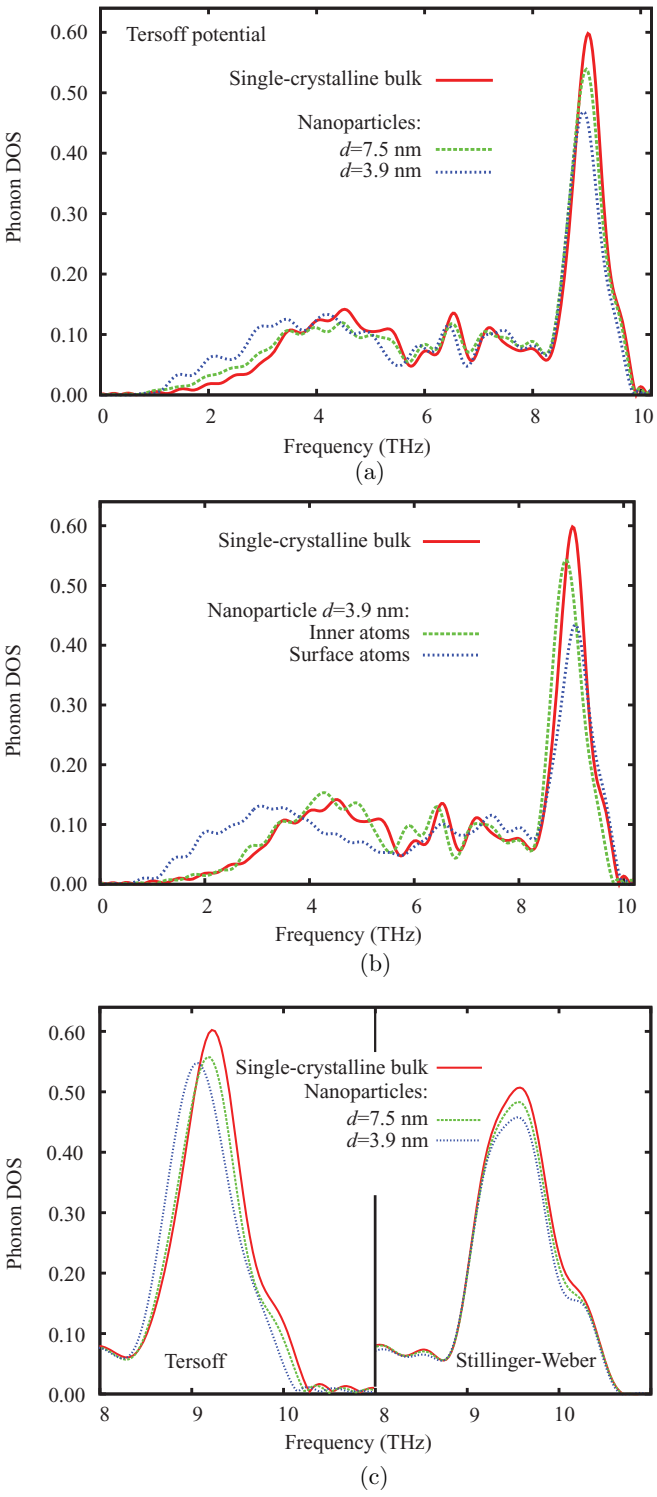

FIG. 2. (Color online) Phonon density of states for crystalline Ge nanoparticles: (a) PDOS of a single crystal compared with the PDOS of nanoparticles with a diameter of $d = 3.9$ and 7.5 nm. (b) PDOS of a single crystal compared with the partial PDOS of the surface and center atoms of a nanoparticle with a diameter of $d = 3.9$ nm. (c) Partial PDOS for the center atoms in nanoparticles with a diameter of $d = 3.9$ and 7.5 nm. The left panel shows the calculation for the Tersoff potential with surface stresses, while the right panel shows the same calculation using the Stillinger-Weber potential without surface stresses and therefore no frequency shift.

of surface atoms also leads to a slight blueshift in the optical modes.

The atoms located in the inner part of the particle, in contrast, exhibit a clear redshift over the entire phonon frequency range. Here, in principle, surface stress or confinement effects could serve as an explanation.[29,30] In order to discriminate between both, we have recalculated the PDOS using another interatomic potential for Ge, namely the Stillinger-Weber format.[21] By construction, this potential has no surface stress and therefore we only expect to see the result of phonon confinement effects. Indeed, the result [see Fig. 2(c)] shows no variation of the peak maximum of the optical modes. Only the shoulder at high frequencies is shifted and can therefore be attributed to a confinement effect due to the lack of vibrational modes close to the Γ point. This can be understood by considering the wave vector $|\vec{q}| \approx \pi/D$, where D is the particle diameter. Small values for q are only possible if D is very large. If D is in the nanometer regime, however, the limiting case $q \to 0$ cannot be reached. Therefore, phonons with q close to zero are missing from the PDOS (see Fig. 9).

In return, the redshift of the optical modes observed with the Tersoff potential can unambigously be attributed to strain effects due to surface stresses. In the case of Tersoff's Ge potential, surface stresses are tensile, leading to a slight lattice expansion corresponding to an increase in interatomic bond length of about 0.1%, which indicates a softening of interatomic force constant. All following calculations are conducted with the Tersoff potential only, since this potential provides a non-negligible and tensile surface stress in line with experimental data.[31–33]

B. Embedded nanoparticles

In the next step, we have studied the role of interface stresses by studying the case of a nanoparticle embedded in a glassy matrix. For this setup, we expect to see an overlap of the contributions of the glassy matrix with the modes of the embedded nanoparticle on which interface stresses are acting.

The bulk glass was prepared by rapid quenching of a melt (quench rate 5 K/ps) leading to an amorphous structure. In the resulting glass, individual particles of different sizes were introduced. This time cubic shapes were chosen, in order to better control the thickness of crystal-glass interfaces. Prior to the PDOS calculations, each structure was again relaxed at 50 K in order to form physically reasonable interfaces between the glass and the particles.

In Fig. 3(a), the PDOS for three different cubic nanoparticles immersed in the glass are displayed and compared with the PDOS of the perfect crystal and the bulk glass. The total number of atoms for all three structures is about 64 000. By decreasing the particle size, we find an increased PDOS in the low frequency and a decreased PDOS at the high frequency peak. The increase of the acoustic modes can be easily explained by the increase of the relative amount of the glassy phase with decreasing crystallite size. The PDOS of a glass displays a characteristic enhancement of the low frequency phonon modes due to the higher volume when compared with the crystalline phase.

Next, we checked if the vibrational modes of the glassy matrix extend into the inner part of the embedded nanoparticle.

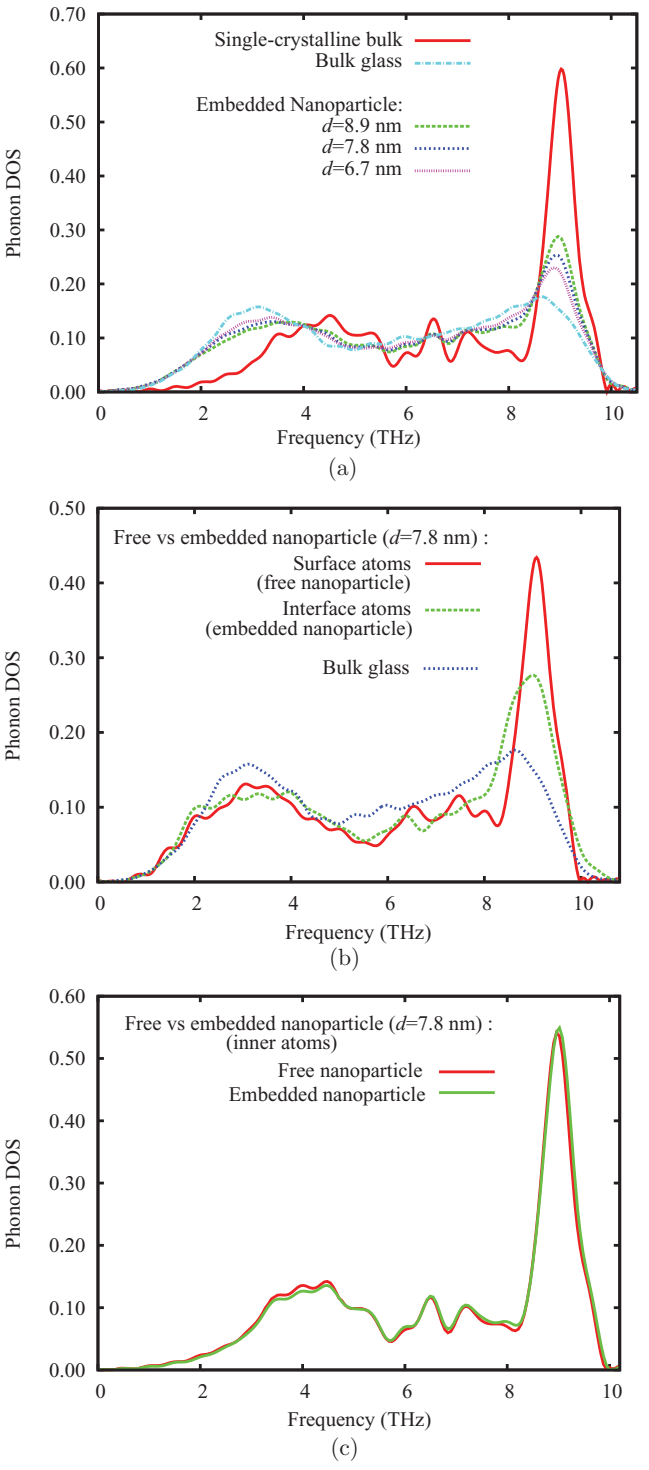

FIG. 3. (Color online) (a) Total PDOS for three different nanoparticles with diameter of $d = 6.7, 7.8$, and 8.9 nm embedded in a glass, as compared to the perfect crystal and the bulk glass. (b)Partial PDOS for interface and surface atoms of an embedded and free nanoparticle, respectively, in comparison to the bulk glass. (c)Partial PDOS for inner atoms of a free and an embedded nanoparticle. In both cases, the nanoparticle size is $d = 7.8$ nm.

For this, the PDOS of an embedded nanoparticle and a free nanoparticle, both with the same geometry and diameter of $d = 7.8$ nm, were calculated. First, we studied how the

glassy matrix affects the PDOS of the crystal-glass interface and compared to the PDOS of the surface and bulk glass. In Fig. 3(b), it can be seen that the partial PDOS of the interface atoms of the embedded nanoparticle differs strongly from the PDOS of the surface atoms of a free nanoparticle and resembles more the PDOS of a bulk glass. This can be explained by the fact that glassy vibrational modes extend in the crystal-glass interfaces. Interface atoms are those that have nearest-neighbor atoms in a diamond-like and glassy configuration, respectively. The calculated partial PDOS of the inner atoms of the embedded and free nanoparticle show no significant difference [Fig. 3(c)]. Therefore, we can conclude that vibrational modes of the glassy matrix do not significantly affect the inner part of the embedded nanoparticle.

In fact, the nanoparticles that are embedded into the glassy structure show also the effect of homogeneous lattice expansion (shift of the PDOS toward lower frequencies). This can be seen from the partial PDOS of only inner atoms of the nanoparticles and as a function of size (Fig. 4). In analogy to the nanoparticle in vacuum, under free surface conditions, the nanoparticles in glass expand due to the interface stress, which also in this case is tensile.

The disappearing shoulder on the main optical peak is again attributable to the confinement effect, which has been discussed in detail in the previous section (see inset in Fig. 4).

C. Nanocrystal

The next setup studied was a nanocrystalline microstructure, which can be understood as an ensemble of nanoparticles connected by "glassy-like" grain boundary areas. All structures were built by means of the Voronoi tesselation method.[34] Samples were prepared with 16 grains of 7.8 nm size, 54 grains of 5.2 nm size, 128 grains of 3.9 nm size, and, finally, 5488 grains of 1.1 nm size. All nanocrystals were initially relaxed at 300 K for 100 ps and then cooled to 50 K prior PDOS calculations.

In Fig. 5(a), we present the PDOS as calculated for these nanocrystals and for the perfect crystal as well as the bulk glass. With decreasing particle size, the maximum of the low frequency region shifts slowly to lower frequencies and the peaks become broader. These features are connected to the ratio between the number of atoms in the grain boundaries and the number of atoms in the bulk-like regions. Due to the higher atomic disorder, the GBs show a signature similar to a glass. Additionally, GBs are characterized by an enhanced free volume preferentially leading to low frequency contributions to the PDOS.

In order to check the validity of our interpretation, we calculated the PDOS separately for atoms in GBs and in the grains. Figure 6(a) shows the partial PDOS for grains with different sizes. As can be seen, the changes of PDOS for the grains in this nanocrystalline structure are essentially identical to the case of the nanoparticles immersed in the glass. Also in this case [inset of Fig. 6(a)], one can easily see the general shift toward lower frequencies with decreasing grain size. As mentioned in the previous section, this behavior is indicative of a tensile interface stress. Previous simulation studies on Cu and Ni[4,10] could not capture shifts in the PDOS with grain size. This is because fcc metals do not exhibit optical modes where

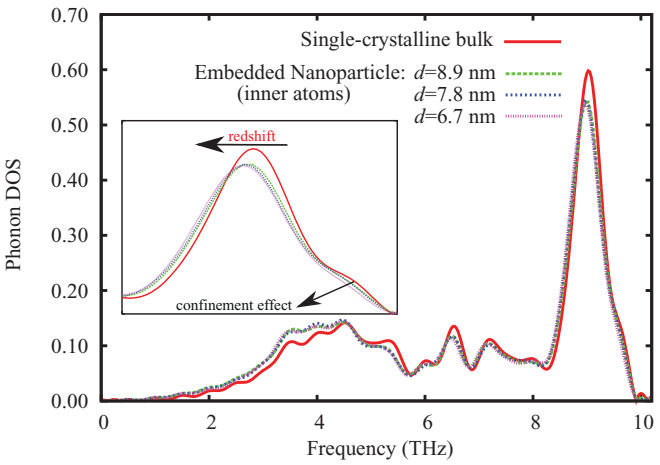

FIG. 4. (Color online) Partial PDOS for different nanoparticles embedded in the glass (only diamond atoms) as compared to the perfect crystal. The inset shows a magnification of the peak of the optical modes.

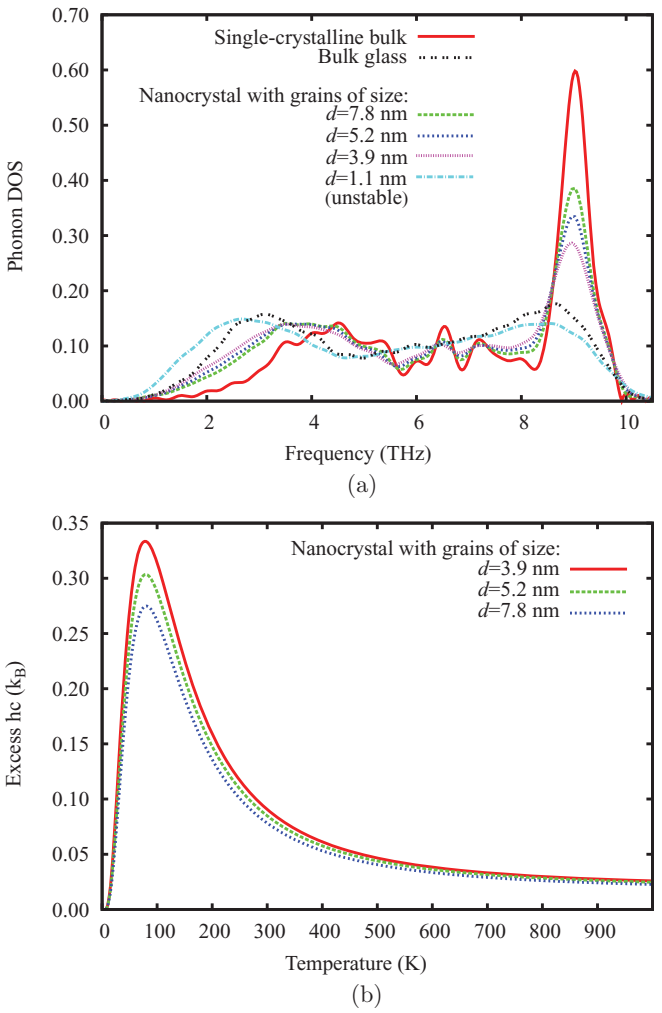

FIG. 5. (Color online) (a) Total PDOS for nanocrystals with different grain sizes as compared to the perfect crystal and a bulk glass. (b) Excess specific heat for three nanocrystals with grain sizes of $d = 3.9$, 5.2, and 7.8 nm, as compared to a bulk crystal.

finite-size effects due to surface stresses and confinement are most prominent. Moreover, the interatomic potentials used in these studies exhibit only a weak compressive surface stress, which has a minor influence on the sparsely populated acoustic modes. This is also the reason why a recent experimental study reported a close similarity of the PDOS of nanograins in nanocrystalline $Fe_{90}Zr_7B_3$ and α-Fe single crystals.[5]

On the other hand, it can clearly be seen that the GBs are the strongest contributors to the increase in the acoustic modes of the PDOS [see Fig. 6(b)] due to a general broadening of the PDOS in those regions. Enhancement of the phonon modes both at low and high energy for GB atoms has been reported earlier also.[5,35]

The increase of the acoustic low frequency modes in the PDOS will cause a direct change in the specific heat and the related thermal properties. In Fig. 5(b), together with the PDOS, we plot the excess specific heat for the three different nanocrystals as compared to the perfect crystal. With decreasing the grain size, or directly increasing the GB fraction, excess low frequency modes will be added, causing an increase in the excess specific heat.

Finally, it should be noted that grain sizes below 1.1 nm lead to unstable grains and result in an amorphous structure. This is in a good agreement with the smallest possible grain size for this material (1–2 nm) observed in experiments.[36,37] The PDOS of this amorphous structure is different from the one calculated for a bulk glass; the acoustic branch is shifted to a lower frequency and is broader. This is due to the excess free volume in the amorphous state. This new structure has an atomic volume of $V_{NC} \approx 24.86$ Å^3, whereas for the bulk glass the atomic volume is $V_{glass} \approx 23.03$ Å^3. The difference is about 8% and in good agreement with our previous results,[18] where we have shown that it is possible to inject an excess free volume up to 8% at room temperature in a Ge glass.

D. Nanoglass

Finally, we have studied the case of a nanoglass. This new type of noncrystalline solid is generated by consolidating

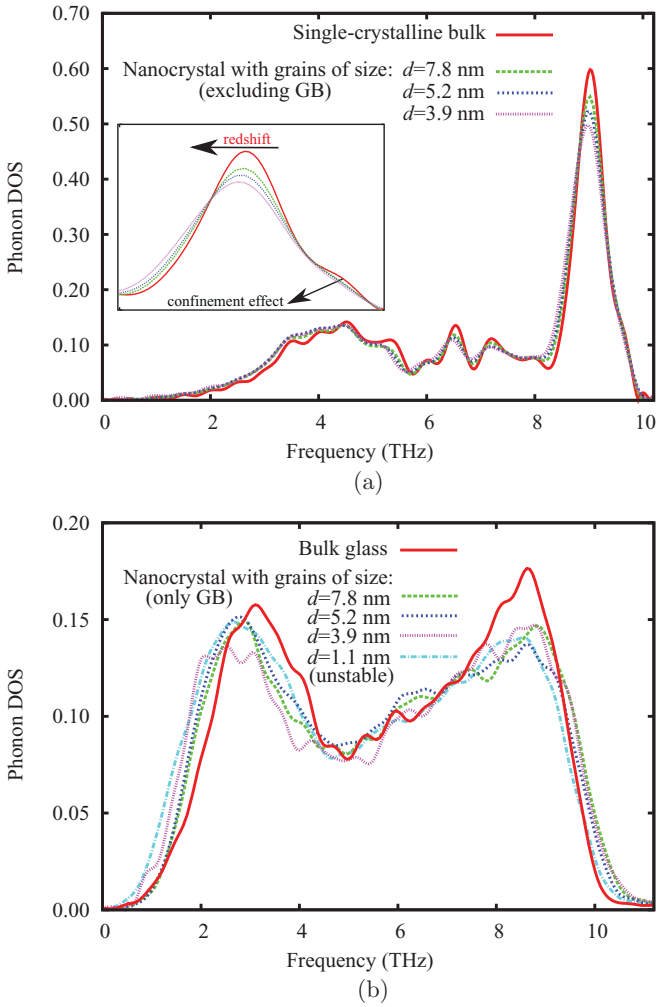

FIG. 6. (Color online) (a) Partial PDOS for three nanocrystals: (a) for grains as compared to the perfect crystal (the inset shows a magnification of the peak of the optical modes) and (b) for GB and resulting amorphous structure of NC with 1.1 nm grains as compared to the bulk glass.

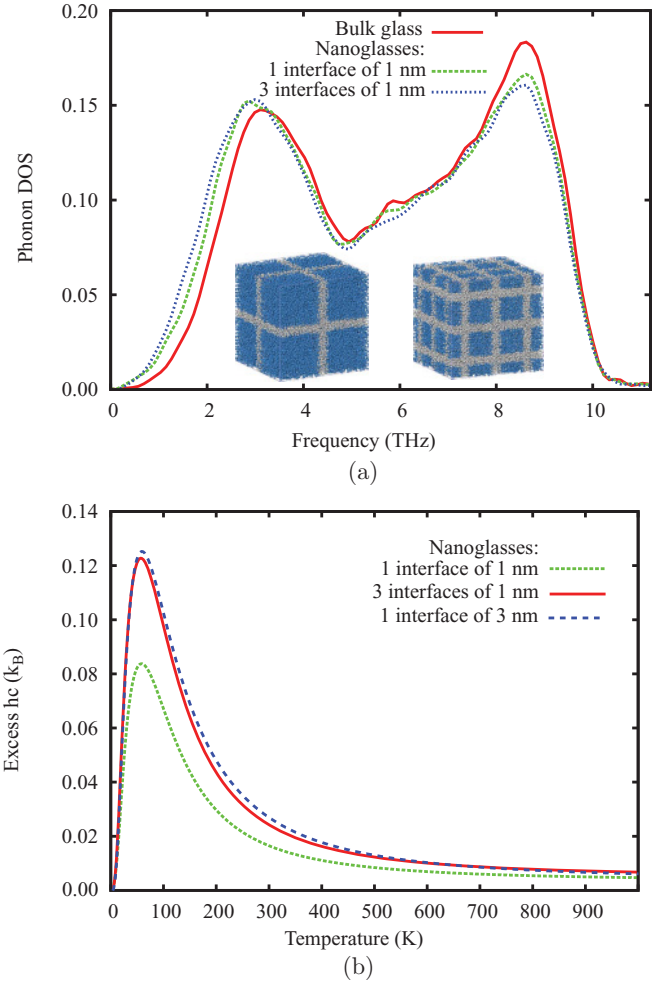

FIG. 7. (Color online) (a) PDOS of a bulk glass compared with the PDOS of two nanoglasses: one with one interface of 1 nm and another with three interfaces of 1 nm. All interfaces have the same percentage of 8% free volume. (b) Excess specific heat for these two nanoglasses and a third nanoglass with one interface of 3 nm as compared to the bulk glass.

nanometer glassy powder, and is characterized by interfaces with an excess free volume.[18] Because this process involves the use of high pressure for powder compaction, also the atomic structure of the inner part of glassy droplets is affected, and in consequence its PDOS is changed compared to the case of bulk glass prepared by rapid quenching of a melt. Therefore, in order to study the size effect on the PDOS as a function of the interface fraction and free volume localized in the interfaces, a simplified glass cubic model (64 000 atoms) with a parallel set of glass-glass interfaces of identical thickness was studied. The interfaces were randomly diluted by 10%, and relaxed at 300 K. The density distribution throughout the sample was monitored during the simulation. After relaxation, interfaces with 8% dilution were found. The calculated interface energy is 1.65 J/m^2.

We calculated the PDOS for two different nanoglass systems. The first one had one interface and the other one three interfaces with the same thickness (1 nm) and the same percentage of 8% free volume. In Fig. 7(a), we see how the acoustic peak shifts to a lower frequency with increasing number of interfaces. The free volume from the interfaces acts as a low frequency source for the phonon modes. In other words, an increase in free volume leads to an increase of low frequency modes in the PDOS. No shifting was observed in the optical modes—only a decrease in the optical peak amplitude due to the PDOS normalization (i.e., with respect to other peaks). This can be explained by a lower interface stress in a nanoglass compared to the interface stress calculated to a nanocrystalline structure. We found no considerable lattice expansion under interface stress and, therefore, we expect no significant change in the PDOS of a nanoglass.

Figure 7(b) shows the related excess specific heat with respect to the bulk glass. It exhibits a pronounced maximum at 80 K, which arises from the acoustic modes with lower frequencies[1] and grows with the number of interfaces. The optical modes provide only a minor contribution to specific heat.

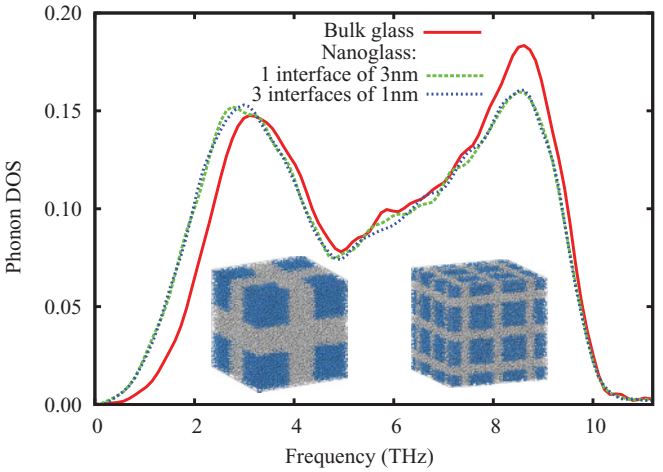

FIG. 8. (Color online) PDOS for bulk glass compared with the PDOS of two nanoglasses, first with one interface of 3 nm and second with three interfaces of 1 nm. All interfaces have the same percentage of 8% free volume. The total amount of free volume is the same for both nanoglasses.

In order to check if phonon confinement depends on the interface thickness in nanoglasses, a similar procedure was followed for two cubic nanoglass structures with the same size; one with one interface of 3 nm and another one with three interfaces of 1 nm. The total free volume was approximately the same in both cases. It can be seen in Fig. 8 that no considerable

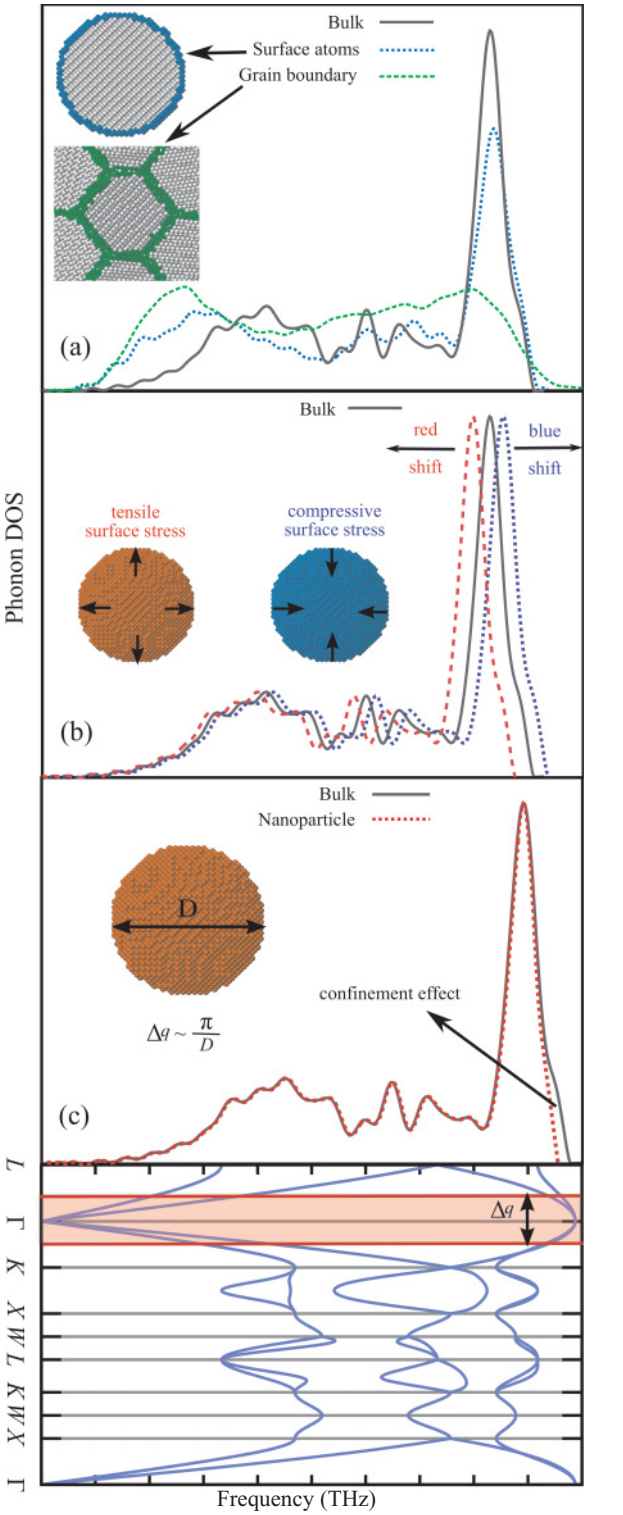

FIG. 9. (Color online) Size effects on PDOS: (a) nanostructural discontinuities; (b) surface stress; (c) confinement due to the particle.

difference in PDOS is observed for these cases. Furthermore, the excess specific heat of the two structures nearly superpose with extremely small differences [see Fig. 7(b)]. This indicates that no extra phonon modes arise from the size effect. In summary, the origin of low frequency phonon modes is only due to the enhanced free volume in the interfaces.

IV. CONCLUSIONS

In this paper, we have investigated the lattice vibrations for different nanostructures for Ge as a prototype of a covalently bonded material. We identified which nanostructural discontinuities affect the phonon modes, realized a complete description of size effects on PDOS, and displayed the specific heat anomaly. We find three size effects (see Fig. 9) that change the PDOS as follows.

(i) Nanostructural discontinuities (surface atoms, GBs, and interfaces) characterized by a lower density in comparison with the bulk crystal cause an enhanced population of acoustical modes with low frequency, and a general broadening of PDOS due to the higher structural disorder.

(ii) Tensile (compressive) surface stresses result in a shift of the entire PDOS to lower (higher) frequencies.

(iii) Confinement due to the finite particle size caused the disappearance of several optical modes at the Brillouin zone center ($q = 0$).

We systematically studied how these three size effects influence the PDOS of different nanostructured materials (nanoparticles, nanocrystals, embedded nanoparticles, and nanoglasses).

Overall, all discontinuities (e.g., GBs, interfaces, and surfaces) in nanostructures will introduce vibrational modes with low frequencies that directly affect the thermal properties of the material. Beside those discontinuities, the PDOS changes also with nanoparticle size through the influence of surface stresses and confinement due to the particle.

ACKNOWLEDGMENTS

The authors acknowledge the financial support of the Deutsche Forschungsgemeinschaft (DFG) through project Al-578-6. A DAAD-PPP travel grant is also acknowledged. Computing time was made available at HHLR Frankfurt and Darmstadt, as well as by CSC Julich. The authors acknowledge Péter Ágoston for fruitful discussions.

*sopu@mm.tu-darmstadt.de

†Present address: Department of Physics, University of Helsinki, P.O. Box 43, FIN-00014 Helsinki, Finland.

[1] D. Wolf, J. Wang, S. R. Phillpot, and H. Gleiter, Phys. Rev. Lett. **74**, 4686 (1995).

[2] C. C. Yang and S. Li, J. Phys. Chem. B **112**, 14193 (2008).

[3] W. S. O. Rodden, C. M. S. Torres, and C. N. Ironside, Semicond. Sci. Technol. **10**, 807 (1995).

[4] P. M. Derlet, R. Meyer, L. J. Lewis, U. Stuhr, and H. Van Swygenhoven, Phys. Rev. Lett. **87**, 205501 (2001).

[5] S. Stankov, Y. Z. Yue, M. Miglierini, B. Sepiol, I. Sergueev, A. I. Chumakov, L. Hu, P. Svec, and R. Ruffer, Phys. Rev. Lett. **100**, 235503 (2008).

[6] A. Valentin, J. See, S. Galdin-Retailleau, and P. Dollfus, J. Phys. Condens. Matter **20**, 145213 (2008).

[7] A. Kara and T. S. Rahman, Phys. Rev. Lett. **81**, 1453 (1998).

[8] H. Richter, Z. P. Wang, and L. Ley, Solid State Commun. **39**, 625 (1981).

[9] L. Pizzagalli, G. Galli, J. E. Klepeis, and F. Gygi, Phys. Rev. B **63**, 165324 (2001).

[10] C. Hudon, R. Meyer, and L. J. Lewis, Phys. Rev. B **76**, 045409 (2007).

[11] R. Shuttleworth, Proc. Phys. Soc. London, Sect. A **63**, 444 (1950).

[12] S. K. Gupta and P. K. Jha, Solid State Commun. **149**, 1989 (2009).

[13] Y.-T. Nien *et al.*, Mater. Lett. **62**, 4522 (2008).

[14] D. S. Chuu, C. M. Dai, W. F. Hsieh, and C. T. Tsai, J. Appl. Phys. **69**, 8402 (1991).

[15] O. O. Mykhaylyk, Y. M. Solonin, D. N. Batchelder, and R. Brydson, J. Appl. Phys. **97**, 074302 (2005).

[16] A. Korotcov, H. P. Hsu, Y. S. Huang, D. S. Tsai, and K. K. Tiong, Cryst. Growth Design **6**, 2501 (2006).

[17] J. Groenen, C. Priester, and R. Carles, Phys. Rev. B **60**, 16013 (1999).

[18] D. Sopu, K. Albe, Y. Ritter, and H. Gleiter, Appl. Phys. Lett. **94**, 191911 (2009).

[19] K. Nordlund, Comput. Mater. Sci. **3**, 448 (1995).

[20] J. Tersoff, Phys. Rev. B **39**, 5566 (1989).

[21] T. A. Weber and F. H. Stillinger, Phys. Rev. B **31**, 1954 (1985).

[22] J. M. Dickey and A. Paskin, Phys. Rev. **188**, 1407 (1969).

[23] R. Yu, D. Singh, and H. Krakauer, Phys. Rev. B **43**, 6411 (1991).

[24] S. Wei and M. Y. Chou, Phys. Rev. B **50**, 2221 (1994).

[25] H. Wang, Chem. Phys. **344**, 299 (2008).

[26] L. J. Porter, J. F. Justo, and S. Yip, J. Appl. Phys. **82**, 5378 (1997).

[27] J. K. Bording and J. Taftoo, Phys. Rev. B **62**, 8098 (2000).

[28] J. D. Honeycutt and H. C. Andersen, J. Phys. Chem. **91**, 4950 (1987).

[29] D. C. Wallace, *Thermodynamics of Crystals* (Dover, Mineola, NY, 1998).

[30] P. Agoston and K. Albe, Phys. Chem. Chem. Phys. **11**, 3226 (2009).

[31] S. Tsunekawa, K. Ishikawa, Z. Q. Li, Y. Kawazoe, and A. Kasuya, Phys. Rev. Lett. **85**, 3440 (2000).

[32] D. Shreiber and W. A. Jesser, Surf. Sci. **600**, 4584 (2006).

[33] M. I. Ahmad and S. S. Bhattacharya, Appl. Phys. Lett. **95**, 191906 (2009).

[34] V. Yamakov, D. Wolf, S. R. Phillpot, and H. Gleiter, Acta Mater. **50**, 61 (2002).

[35] A. Kara, A. N. Al-Rawi, and T. S. Rahman, J. Comput. Theor. Nanosci. **1**, 216 (2004).

[36] T. Nieh and J. Wadsworth, Scr. Metall. Mater. **25**, 955 (1991).

[37] L. L. Araujo, R. Giulian, D. J. Sprouster, C. S. Schnohr, D. J. Llewellyn, P. Kluth, D. J. Cookson, G. J. Foran, and M. C. Ridgway, Phys. Rev. B **78**, 094112 (2008).